Research Square

Preprints are preliminary reports that have not undergone peer review.
They should not be considered conclusive, used to inform clinical practice,
or referenced by the media as validated information.

Response surface methodology approach for dyeing process optimization of Ayous (Triplochiton scleroxylon) wood with acid dye

Shiqian Wu
Research Institute of Wood Industry, Chinese Academy of Forestry
Limin Peng (penglm@caf.ac.cn)
Research Institute of Wood Industry, Chinese Academy of Forestry
Feng Fu
Research Institute of Wood Industry, Chinese Academy of Forestry
Yun Feng
Research Institute of Wood Industry, Chinese Academy of Forestry
Jinrong He
Research Institute of Wood Industry, Chinese Academy of Forestry
Huishan Wang
Research Institute of Wood Industry, Chinese Academy of Forestry

Research Article

Keywords: Response surface methodology, Triplochiton scleroxylon, Process optimization, Dye penetration rate

Posted Date: October 4th, 2022

DOI: https://doi.org/10.21203/rs.3.rs-2026272/v2

License: This work is licensed under a Creative Commons Attribution 4.0 International License. Read Full License

Additional Declarations: No competing interests reported.

Version of Record: A version of this preprint was published at European Journal of Wood and Wood Products on March 2nd, 2023. See the published version at https://doi.org/10.1007/s00107-023-01939-2.

Abstract

Dyeing of wood is an important value-adding process. An important indicator in the assessment of the performance of wood dyeing process is the dye penetration. In present study, the existing method of response surface methodology was extended to study the dyeing process optimization of Ayous (*Triplochiton scleroxylon*) wood with acid dye using the radial dye penetration rate as an indicator. The experiments were carried out on the basis of a single factor experiment, and the optimal condition was determined by means of the Box-Behnken Design of response surface methodology. The effects of temperature, dye concentration, dyeing time and accelerant mass fraction on the radial dye penetration rate of Ayous wood were optimized. The experimental results showed that the maximum radial dye permeability can be achieved under optimum dyeing temperature (86.03 ^{o}C), dye concentration (0.31%), dyeing time (8 h), and accelerant mass fraction (2.23%). Under these conditions, the maximum dye-uptake and radial dye penetration rate were found to be 14.28% and 22.34%, respectively. The results of analysis of variance indicated that the mathematical model proposed in this study can be used to predict the dye-uptake and radial dye penetration rate of acid dye on Ayous wood by changing the process parameters.

Introduction

As one of the materials that have the closest relationship with human beings and the most harmonious development with the environment, wood and wood-based materials are ubiquitous for the millennium in the development of building and furniture of the human living environment, due to their good material properties and environmental characteristics (Hu et al., 2020; Ndukwu et al., 2021). Compared with other commonly used modern engineering materials, such as steel, concrete and plastic, wood has the advantages of high strength-to-weight ratio, good elasticity, easy processing, natural beautiful texture and color, and renewable ability (Bao et al., 2016; Borrega et al., 2015; Knudson and Brunette, 2015; López et al., 2018; Yang et al., 2019; Liu et al., 2021a). The uneven color and “dull appearance” of wood are important factors affecting its utilization and commercial value. These visual defects can be eliminated by color modulation techniques such as bleaching, dyeing, etc. to improve the decorative properties of wood (Nguyen et al., 2018a). At the same time, dyeing allows low-quality wood to imitate the color of natural precious wood, so dyeing of wood has always been a vivid field of research and development in wood processing (Jaxel et al., 2020).

Dyeing is an important value-adding process from an industrial perspective. Generally, wood dyeing mainly uses dyes (acid dyes, basic dyes, etc.) to achieve the desired color. The dye molecules enter the wood through the multilevel infiltration channels of wood cells, and are adsorbed, set and fixed into wood fibers or tracheids by intermolecular van der Waals and hydrogen bonding forces (Liu et al., 2015; Liu et al., 2020). The quality of dyed wood and dyeing depth depend on the degree of absorption and penetration of dye molecules into the wood structure. However, with the exception of longitudinal tracheids that are naturally quite permeable in the direction in which fluids must flow, there are limited tangential and radial channels available for dye penetration. Comstock (2007) calculated the directional permeability of softwoods based on the available gas permeability data and found that the ratio of longitudinal to tangential permeability varies from 520 to 81,600, and the longitudinal to radial ratio varies from 15 to 547,000. The tangential and radial penetration of the wood is related to the dyeing depth, and in general, as the thickness of the wood increases, it becomes more difficult for dyes to penetrate (Rowell, 2012).

Atmospheric pressure impregnation is a simple and mature technology, in which expensive high-pressure reactors are not essential, so it is the most commonly used method for wood dyeing at present. The effect of atmospheric dyeing is directly affected by the process parameters, such as dye concentration, temperature, dyeing time, dosage of accelerant and so on. Depending on the dyes and tree species, different dyeing parameters should be adopted (Wang et al., 2017; Wang et al., 2018b). Hu et al. (2016) studied the influence of dyeing parameters on the dye-uptake and color difference of *Acer saccharum* veneer, showed that the dye concentration and dyeing temperature had the greatest effect by visual means and analysis of variance, and obtained the optimal process by fuzzy synthetic evaluation. Nguyen et al. (2018b) investigated the types of dye (direct dye and reactive dye) and dyeing parameters (dye concentration, dyeing time, and temperature) in the veneer dyeing process for *Eucalyptus globulus*, and showed that the reactive dye Procion Brown P2RN at a concentration of 2% resulted in a highest dye penetration.

Ayous (*Triplochiton scleroxylon*), also known as Obeche, is an important species from the tropical forests in West and central African, especially in Equatorial Guinea, Cameroon and Gabon. It is a large deciduous tree growing up to 50 m in height and up to 1.5 m in diameter (Jardine et al., 2016; Nouemsi Soubgui et al., 2021; Togue Kamga, 2018). The timber from Ayous possesses unique intrinsic features, such as uniform material properties, high processability, small drying shrinkage and few appearance defects that have led to it being widely used in the production of multilaminar decorative lumber (MDL). In the current MDL research, the dye-uptake is mostly selected as the criteria to evaluate the Ayous wood veneer dyeing process, but there is little attention has been paid to the dye penetration. Meng et al. (2016b) shows that increasing the thickness of veneer can significantly save glue consumption, thereby reducing production costs and environmental pollution (Meng et al., 2016a). To achieve an optimal dyeing process of thicker veneer, the relationship between dyeing parameters and dye penetration must be determined.

The response surface methodology (RSM) is a set of mathematical techniques that investigates the effective parameters on a response. It mainly includes three steps of experimental design, model construction, and data analysis, then evaluates the interactions between the response factors to determine the optimal conditions (Antony, 2014; Hazir and Ozcan, 2019; Singh et al., 2016). This technique can be used especially for improving efficiency of the processes. Compared with the traditional univariate method and orthogonal experiment method, RSM can establish a multiple quadratic regression equation containing the factors and the response values, thereby presenting an advantage in clarifying the interaction between variables (Khataee et al., 2011; Witek-Krowiak et al., 2014). Besides that, this design also has several advantages such as a minimum number of experiments required, data analysis applied using three-dimensional graphs (Ghaedi et al., 2016; Das and Mishra, 2017; Yusop et al., 2021), so it has been widely used as a technique for designing experiments since it was developed by Box and Wilson (1951).

Recent studies have shown that RSM has also been selected as a design of experiment for optimizing process parameters to achieve higher dyeing effect of wood (Deng et al., 2019). Though, very few reports are available on using dye penetration to evaluate the effect of Ayous wood staining. Science, dye penetration is important and realistic for Ayous thicker veneers. Our study has been comprehensively focused on the same to fill this research gap in the field of Ayous staining. This present paper assesses the performance of Ayous wood under different dyeing processes parameters, especially the dye penetration. By using response surface methodology (RSM), the optimum dyeing conditions of temperature, dye concentration, dyeing time and accelerant mass fraction were determined. This study will provide technical guidance and theoretical support for the production of dyed Ayous thick veneers.

Materials And Methods

Materials

The Ayous (*Triplochiton scleroxylon*) wood used in this study was purchased from Shenghuayunfeng New Materials Co., Ltd. in Deqing, Zhejiang Province. The raw material consisted of sapwood with a low density (ρ = 0.33–0.48 g/cm^3) and an initial dry moisture content of 10–12%. The initial color parameters of Ayous in the CIE 1976 $L^*a^*b^*$ homochromatic space were as follows: lightness (L^*) 76.71 ± 1.12, red-green chromaticity index (a^*) 6.02 ± 0.36, and yellow-blue chromaticity index (b^*) 27.26 ± 0.62. Each sample with a size of 10 mm × 10 mm × 50 mm (radial (R) × tangential (T) × longitudinal (L)) were sawn from the defect-free parts of the Ayous log for dyeing tests of different processes. Three aryl methane Acid Blue V (*C. I. Acid Blue 1*) (ABV) dye which is commonly used in the wood dyeing industry was provided by Hengsheng Chemical Co., Ltd., in Hangzhou. The molecular formula is illustrated in Fig. 1. Anhydrous sodium chloride was acquired from Tianjin Kemeiou Chemical Reagent Co., Ltd. All the other chemicals were obtained from Sinopharm Chemical Reagent Beijing Co., Ltd. and were reagent grade.

Dyeing methods

An atmospheric pressure dip-dyeing method was used for wood dyeing. The dye-uptake of the dye liquor and dyeing depth of the dyed samples were examined. The effect of temperature, concentration of dye liquor, dyeing time, and dosage of accelerant on the properties of dyed wood was investigated afterwards.

Acid Blue V dye liquor 0.1%, 0.2%, 0.3%, 0.4%, 0.5% (w/w) was prepared and 0, 1.0%, 2.0%, 3.0%, 4.0% (w/w) anhydrous NaCl were added as an accelerant. The dyeing process was carried out at 65 ^{o}C, 75 ^{o}C, 85 ^{o}C and 95 ^{o}C with oridinary pressure for 2, 4, 6, 8 or 10 h, respectively. The pH value of the dye liquor was adjusted to 4.0 by 10% H_2SO_4 (w/w) or 10% NaOH (w/w). For each condition, four wood were placed in a beaker, leaving gaps between the wood so as to ensure adequate contact between the samples and the dye solution. The bath ratio was 1:20 (V_{wood}:$V_{dye\ liquor}$). After dyeing, the raffinate of all the samples were washed away by tap water, and then the moisture content was air-dried to 12% in a cool place without light. The dye-uptake and dye penetration rate of the dye liquor and chromatic value of the dyed samples was measured before and after the experiment.

Color parameters

The chromaticity value is the simplest and most direct parameter to indicate the significant effect of dyed wood on the process method. The difference of color parameters directly determines the visual effect and commercial value of the wood. Color parameters including L^*, a^*, and b^* were measured by Benchtop CR-400 colorimeter (Konica Minolta, Japan) under the operation conditions, *i.e.* D65 standard illuminant and 0/d vertical illumination/diffuse reflection. The sample was measured three times at different positions. For each group, four samples were measured and the averages of the four were reported. The total color difference ΔE (expressing the distance between two points in the CIE 1976 $L^*a^*b^*$ homochromatic space) was calculated from Equations (1–4) (Machová et al., 2019; Liu et al., 2021b; Zhu et al., 2021):

$$\Delta L^* = L_1^* - L_0^* \quad (1)$$

$$\Delta a^* = a_1^* - a_0^* \quad (2)$$

$$\Delta b^* = b_1^* - b_0^* \quad (3)$$

$$\Delta E = [(\Delta L^*)^2+(\Delta a^*)^2+(\Delta b^*)^2]^{1/2} \quad (4)$$

Where ΔE indicates the degree of total color change after dyeing, L^* axis represents the lightness/darkness of the dyed wood ranging from 0 (black) to 100 (white); a^* axis stands for redness/greenness of the dyed wood, with positive (+) indicating red and negative (-) representing green; and the b^* axis specifies the ratio of yellow (positive) to blue (negative). L_0^*, a_0^*, and b_0^* are the parameters measured for the control; L_1^*, a_1^*, and b_1^* are the parameters measured after dyeing, respectively.

Measurement of dye-uptake

Dye-uptake is one of the most important parameters for the wood dyeing process because it affects the quality of dyed wood and dye absorption. Measurement of dye-uptake was carried out by different methods in various studies on different materials (Deng and Liu, 2010; Zhang et al., 2015). In this study, the dye-uptake was calculated according to the Beer-Lambert law to determine the relationship between the dye concentration and absorption. The S54 spectrophotometer (Lengguang, China) was used for evaluating the absorption of dyes, which the maximum wavelength (λ_{max}) was at 638 nm. The dye-uptake (U, %) can be obtained based on Eq. (5).

$$U\% = 100 \times (A_0 - A_1)/A_0 \quad (5)$$

Where A_0 and A_1 represents the absorbance of the dye solution at λ_{max} before and after dyeing, respectively.

Radial dye penetration rate test

To achieve an optimal wood dyeing process, dye penetration was established as an important criteria for selection of suitable dyeing parameters. The dyed wood was evenly separated along the transverse and cut into 3 pieces. The radial minimum depth of the dye penetration on the left and right sides of the second piece were measured, and the average value was the radial dyeing depth of the sample (Fig. 2). The radial dye penetration rate (W, %) was calculated by Eq. (6).

$$W\% = 100 \times (H_1 + H_2 + H_3 + H_4 + H_5 + H_6 + H_7 + H_8)/(4H) \quad (6)$$

Where H_1 - H_8 represents the depth of the dye solution penetration, mm; H was the radial length of the sample, mm.

RSM approach of experimental design

The Box-Behnken design (BBD) was chosen as the experimental design. This method is suitable for fitting a quadratic surface (Ryan, 2007). The BBD is effective in optimizing parameters with a minimum number of experiments, and also useful in analyzing the interaction between the parameters (Azargohar and Dalai, 2005). The independent variables selected for this experiment were temperature (X_1), dye concentration (X_2), dyeing time (X_3) and accelerant mass fraction (X_4). These four variables and their ranges were chosen based on a single-factor analysis before designing this experiment, the factor codes and levels were shown in Table 1. The dye-uptake and radial dye penetration rate were measured. With five replicates at the center point, the BBD for four independent variables was a total number of 29 experiments as calculated in Eq. (7).

$$N = 2k\times(k-1) + n_c = 2\times4\times(4-1) + 5 = 29 \quad (7)$$

Where N is the total number of experiments, k is the number of independent variables and n_c is the number of central points.

Table 1
Independent variables and their coded levels for the Box-Behnken design

Level	Factors			
	X_1	X_2	X_3	X_4
	Temperature (°C)	Dye concentration (w%)	Dyeing time (h)	Accelerant mass fraction (w%)
-1	75	0.2	6	1
0	85	0.3	8	2
1	95	0.4	10	3

In this research, the Design Expert 12.0.3 software (Stat-Ease, USA) was utilized. The quadratic polynomial model was used to investigate the effects of factors. Analysis of variance (ANOVA) was used to make adequate the developed models through the observed data.

Results And Discussion

Effect of temperature on wood dyeing

Under the conditions of dye concentration of 0.2%, dyeing time of 4 h, and accelerant mass fraction of 1%, the relationship between increased temperature and dye-uptake, radial dye penetration rate and color parameters of the dyed wood was demonstrated by Fig. 3. It can be found from the Fig. 3a that the dyeing temperature has a certain positive effect on the dyeing of Ayous wood. When the temperature was 65 °C, the dye-uptake was 5.66%, and it increased slightly with the increase of temperature. At 85 °C, the dye-uptake reached a maximum of 7.80%. Increasing temperature made the dye molecules get more energy, and the movement of the dye molecules was accelerated, which increased the probability of the collision between the dye and the wood to form van der Waals forces and hydrogen bonds (Liu et al., 2015). Moreover, the amorphous area within wood fibers increased along with temperature, thus allowing more dye molecules to be adsorbed, diffused and fixed in wood fibers (Wang et al., 2017; Song and Shen, 2009). When the temperature continued to rise to 95 °C, the dye-uptake decreased slightly, which was mainly due to the desorption of the adsorbed dye molecules with the excessively high temperature (Wang et al., 2018a). At the same time, high temperature made a strong affinity of dyes and wood surface, which may cause dyes to be adsorbed on the orifice of capillary, forming triangular adsorption and hindering further diffusion of dyes (Zhao et al., 1993).

As can be seen from Fig. 3a, the increase of dyeing temperature has obvious positive effect on the improvement of dye penetration rate. When the temperature was 65 ^{o}C, the dye penetration rate was 8.77%, and the value increased significantly with the increase of temperature. When the temperature rase to 95 ^{o}C, the dye penetration rate reached 14.87%, which is 1.70 times of that at 65 ^{o}C. This was because the increase of temperature improved the activation energy of the dye molecules, which is the ability of dye molecules to penetrate from surface to interior of the wood fibers (Vakhitova and Safonov, 2003). When dye anions were transferred to fibers, they must move with their own sodium ions to maintain electrical neutralization. However, the concentration of sodium ions near the fiber interface was much higher than that in the dye liquor, so it would take energy to transfer sodium ions from the area with low concentration to high concentration. In addition, increasing the temperature could significantly reduce the aggregation degree of dyes, thereby improving the diffusion properties of dye molecules (Lv et al., 1994; Li et al., 2011).

The effect of dyeing temperature on the surface color of Ayous wood is shown in Fig. 3b. The changes of lightness, red-green index and yellow-blue index of dyed wood had a certain correlation with the changes of dye-uptake. Generally speaking, as the dye-uptake rose, the adsorption of ABV dye on the wood surface increased, the L^* became lower, while the a^* and b^* were higher. Wood dyed at 85 ^{o}C had the highest dye-uptake, the lowest L^* (30.57), and the highest a^* (-14.08) and b^* (-20.32). However, in the range of 65–95 ^{o}C, the difference between the maximum and minimum of dye-uptake was only 2.14%, so the surface total color difference ΔE only changed by 2.53 NBS (from 66.73 NBS to 69.26 NBS). According to the relationship between color difference and people visual recognition, when ΔE is in the range of 1.5–3.0 NBS, the color difference was only perceptible (Duan, 2002). Dyeing temperature had no significant effect on surface color difference.

Effect of dye concentration on wood dyeing

Figure 4 shows the trends of dye-uptake, dye penetration rate and color parameters as a function of dye liquor concentration. Different dye concentrations had different results of dye-uptake. When the concentration of dye solution was 0.1%, the dye-uptake was 7.16%. The dye-uptake increased rapidly as the concentration grew, and the highest value was 10.79% at 0.3% concentration. Then, continuing to expand the concentration would result in decreased uptake, and the dye-uptake was 6.48% when the concentration reached 0.5%. The enlargement of the concentration means that the number of dye molecules in the dye liquor increases, and dye contacts and collides with the wood fiber surface more frequently. When the concentration reached a certain degree, the adsorption of dyes on wood arrived at saturation state. After the absolute adsorption amount was stable, the increase of concentration would naturally reduce the dye-uptake.

The change of dye penetration rate showed a similar trend with dye-uptake. With the dye concentration was 0.1%, the dye penetration rate was 11.13%. An increased permeability occured before the concentration reaches 0.4%. Subsequently, improving the dye concentration resulted in a diminution of dye penetration. At low concentrations, more dye molecules represent more opportunities for exposure of dyes to wood. However, at higher concentrations, the dye molecules were seriously aggregated. It was difficult for the aggregates to flow and diffuse in the wood. The movement resistance of dye molecules increased, and the diffusion speed was slowing down. and even will cause color degradation. Excessive concentrations could even cause insoluble dye deposits on the surface of the wood.

As shown in Fig. 4b, with the increase of dye concentration, the lightness value and the yellow-blue index of dyed wood surface gradually decreased, while the red-green index gradually increased. The results showed that the color of wood surface was deepened, and shifted towards red and blue when the dyeing concentration got larger. When the mass fraction of dye spread from 0.1–0.5%, the total color difference on the wood surface gradually increased, and the maximum value was 73.25 NBS. Due to the enlarged number of dye molecules adsorbed and aggregated on the wood surface, the promotion of dye concentration results in more pronounced color difference. The ΔE of dyed sample at 0.5% concentration changed by 4.83 NBS compared with that dyed at 0.1% concentration. When ΔE is in the range of 3.0–6.0 NBS, the color difference can be recognized by the human visual system. This result shows that the dye concentration had a significant effect on the surface color difference.

Effect of dyeing time on wood dyeing

Figure 5 shows the influence of dyeing time on dye-uptake, dye penetration rate and color parameters. As shown in Fig. 5a, the dye-uptake gradually increased until the dyeing time exceeded 8 h. The dye-uptake value of 10 h dyed wood was 9.57%, which was less than the value of 10.48% at 8 h. Dyeing is a slow process in which dye molecules adsorb to the wood surface, diffuse and penetrate into the wood, and finally precipitate on the wood fiber (Convert et al., 2000; Mikhailovskaya et al., 2001). In the process, adsorption and desorption existed simultaneously. At the initial stage of dyeing, the degree of adsorption was greater than that of desorption, so the whole action was dominated by adsorption, and the dye-uptake increased with time. When the dye-uptake reached the maximum, desorption became the mainly action. With the extension of dyeing time, some dye molecules adsorbed on wood fiber might be desorbed, caused a decrease in dye-uptake.

It can be seen from the figure that dyeing time had a positive effect on dye permeability. The dyeing time ranged from 2 to 10 hours, the radial dye penetration rate of Ayous wood increased from 9.53–17.90%. During the dyeing process, the dye quickly penetrated into the interior of wood, and the dye penetration rate rase significantly in the first 6 hours. Over 8 hours, this trend gradually slowed down. Since the structure and chemical composition of wood are different from cotton and linen textiles, the dyeing of wood with dyes is a gradual and slow process. Due to the thickness of the sample, the resistance of the dye to diffuse into the wood would become greater and greater, the penetration of the dye would become more and more difficult. Therefore, the longer the dyeing time, the smaller increase in dye penetration.

As shown in Fig. 5b, dyeing time had little effect on wood surface color parameters. In the dyeing time range of 2–10 h, the change range of L^* value was from 27.05 to 31.51, the change range of a^* value was from − 12.70 to -15.83, the change range of b^* value was from − 18.86 to -23.60, and the change range of total color difference ΔE was from 68.75 NBS to 71.91 NBS. Except for the 8 h dyed sample, there was no obvious color difference between the remaining wood. The dyeing time had little influence on color difference, which was consistent with previous research results (Chen et al., 2000).

Effect of accelerant mass fraction on wood dyeing

Figure 6 shows the influence of accelerant mass fraction on dyeing performance. As can be seen from Fig. 6a, the dye-uptake increased obviously after adding accelerant, the addition of NaCl had a significant promotion effect on the adsorption of dyes. When the mass fraction was 1%, the dye-uptake was 7.80%, which was 2.19 times of that without NaCl. Compared with 0% concentration, adding 2% NaCl could improve the dye-uptake by 2.74 times. NaCl in dye liquor would be ionized into sodium ions and chloride ions. Studies have shown that wood has negative charge in dye liquor. Therefore, sodium ions would be attracted by the negative charge of wood, while chloride ions would be repelled. Under the shielding effect of sodium ions, the repulsive force of dye anions on wood surface was greatly weakened, thus improving the dye-uptake. However, excessive accelerant concentration would cause the aggregation of dye molecules and even dye precipitation, decreasing the dye-uptake.

The dye penetration rate showed similar trends with dye-uptake. When the concentration of NaCl was 2%, the dye penetration rate reaches the maximum value of 16.83%. The results showed that the increase of NaCl could enlarge the diffusion boundary layer on wood surface and promote dye diffusion into wood at lower accelerant concentration. Increasing the concentration of NaCl would cause the aggregation and precipitation of dye molecules. The movement resistance of dye molecules got bigger after aggregation, and it was difficult for the aggregates to flow and diffuse in wood. Therefore, excessive NaCl was not conducive to dye penetration.

The effects of different mass fractions of NaCl on the surface color parameters of Ayous wood are shown in Fig. 6b. Compared with the dyed wood without NaCl, the value of L^* and b^* were lower, and the a^* was higher of the samples with NaCl addition, and the ΔE was also higher. With the change of NaCl content, the total color difference increased at first and then decreased. When the concentration of NaCl was 3%, the ΔE was 73.26 NBS. The reason for the above changes was that NaCl as an accelerant weakened the Coulomb force between the wood fiber and dye anions. It was beneficial to the adhesion and combination between wood and dyes, thereby increased the dye-uptake and color difference. If the amount of accelerant continued to increase, the dye molecules would self-polymerize, which was not conducive to dyeing, so the color difference value would be reduced.

RSM model establishment and significance test

Table 2 shows the results of BBD experiments in studying the combined effect of four independent variables with different combinations along with the experimentally observed and predicted values of dye-uptake and dye penetration rate of Ayous wood. According to Table 2, the highest dye-uptake (14.48%) was achieved for actual data in standard order 18 and the highest dye penetration rate (22.43%) was achieved in standard order 6. Coincidentally, both results were achieved under the same conditions, that is, temperature 85 ^{o}C, dye concentration 0.3%, dyeing time 8 h, and accelerant mass fraction 3%.

The experimental data were analyzed using analysis of variance (ANOVA), the results indicated that the established model was significant. The dye-uptake and dye penetration rate were quadratic polynomial functions of four parameters studied in Table 2. The R^2 value of the developed model of dye-uptake and dye penetration rate was found to be 0.985 and 0.982, respectively, and the adjusted R^2 was 0.970 and 0.963, respectively. These values of the correlation coefficients were close to the ideal and statistically acceptable to establish the relationship between the experimental and predicted values (Ahmad and Hameed, 2010). The predicted R^2 (Pred. R^2) of dye-uptake and dye penetration rate were 0.936 and 0.909, respectively, which were in reasonable agreement with R^2 and adjusted R^2. Measuring the adequate precision can estimate the signal-to-noise ratio, and an adequate precision greater than 4.0 is acceptable (Danish et al., 2014a). The values of adequate precision (Adeq. Precision) of dye-uptake and dye penetration were 26.74 and 27.68, respectively, and were high enough to guarantee the accuracy of the experiment. Therefore, the proposed model can be used to predict experimental results.

Tab. 2 Experimental design and results of the response surface analysis

Run	Factors				Responses					
	X_1	X_2	X_3	X_4	Y_1			Y_2		
					Actual	Predicted	Residual	Actual	Predicted	Residual
1	85	0.4	8	3	12.78	12.70	0.08	19.59	19.75	-0.16
2	95	0.4	8	2	12.67	12.77	-0.10	20.50	20.66	-0.16
3	85	0.2	8	1	10.48	10.50	-0.02	17.60	17.18	0.42
4	85	0.3	10	1	11.13	11.22	-0.09	15.43	15.52	-0.09
5	75	0.3	8	3	12.27	12.34	-0.07	19.47	19.53	-0.06
6	85	0.3	8	2	14.15	14.18	-0.03	22.43	22.11	0.32
7	95	0.3	8	3	12.07	12.07	0.00	20.13	19.64	0.49
8	75	0.3	6	2	11.62	11.48	0.14	17.07	17.01	0.06
9	95	0.3	8	1	11.29	11.09	0.20	18.86	18.93	-0.07
10	85	0.3	10	3	11.94	11.88	0.07	19.87	19.95	-0.08
11	85	0.4	6	2	12.42	12.24	0.18	19.05	19.13	-0.08
12	95	0.3	10	2	11.44	11.52	-0.08	19.18	18.98	0.20
13	95	0.3	6	2	11.92	11.98	-0.06	19.80	19.83	-0.03
14	85	0.3	8	2	13.87	14.18	-0.31	22.11	22.11	0.00
15	75	0.3	8	1	11.10	10.97	0.13	14.02	14.63	-0.61
16	85	0.3	8	2	14.48	14.18	0.30	21.63	22.11	-0.48
17	85	0.4	10	2	12.65	12.62	0.03	18.50	18.79	-0.29
18	85	0.3	8	2	14.23	14.18	0.05	22.35	22.11	0.24
19	85	0.3	8	2	14.19	14.18	0.01	22.04	22.11	-0.07
20	85	0.3	6	1	10.33	10.59	-0.26	17.34	17.39	-0.05
21	95	0.2	8	2	11.27	11.23	0.04	19.92	20.35	-0.43
22	85	0.3	6	3	12.18	12.28	-0.10	18.52	18.57	-0.05
23	85	0.2	6	2	11.58	11.48	0.10	19.42	19.26	0.16
24	75	0.3	10	2	12.30	12.17	0.13	17.68	17.38	0.30
25	75	0.2	8	2	11.73	11.82	-0.09	18.70	18.68	0.02
26	85	0.2	10	2	11.27	11.32	-0.05	19.08	19.12	-0.04
27	75	0.4	8	2	12.11	12.34	-0.23	18.21	17.92	0.29
28	85	0.2	8	3	11.99	11.97	0.02	20.82	20.96	-0.14
29	85	0.4	8	1	11.86	11.82	0.04	18.34	17.94	0.40

The statistical significance of the proposed quadratic model for both the responses was evaluated by ANOVA and corresponding F-values and the values of “Probability > F” (p-value). For statistically significant model terms, the p-value less than 0.05 indicates that the model is significant, and the p-value less than 0.01 indicates that the model is extremely significant (Amini and Younesi, 2009). For both responses of dye-uptake and dye penetration rate, the quadratic model was selected, as suggested by the software. By using multiple regression analysis, the responses (dye-uptake and dye penetration rate) were correlated with the four variables studied using the second-order polynomial (Danish et al., 2014b). For this model, development of the main effects, square effects and interaction effects of the temperature, dye concentration, dyeing time, and accelerant mass fraction were statistically evaluated and are reported in Table 3.

Tab. 3 Variance analysis of the regression model for dye-uptake and dye penetration rate

Source	Sum of Squares		df		Mean Square		F-value		p-value		Significant	
	Y_1	Y_2	Y_1	Y_2	Y_1	Y_2	Y_1	Y_2	Y_1	Y_2	Y_1	Y_2
Model	33.39	104.56	14	14	2.38	7.47	64.9	52.92	< 0.0001	< 0.0001	**	**
X_1	0.0184	14.61	1	1	0.0184	14.61	0.5009	103.5	0.4907	< 0.0001		**
X_2	3.17	0.1519	1	1	3.17	0.1519	86.32	1.08	< 0.0001	0.3172	**	
X_3	0.0385	0.1776	1	1	0.0385	0.1776	1.05	1.26	0.3232	0.2808		
X_4	4.13	23.55	1	1	4.13	23.55	112.39	166.84	< 0.0001	< 0.0001	**	**
X_1X_2	0.2601	0.2862	1	1	0.2601	0.2862	7.08	2.03	0.0186	0.1763	*	
X_1X_3	0.3364	0.3782	1	1	0.3364	0.3782	9.15	2.68	0.0091	0.1239	**	
X_1X_4	0.038	4.37	1	1	0.038	4.37	1.03	30.95	0.3263	< 0.0001		**
X_2X_3	0.0729	0.011	1	1	0.0729	0.011	1.98	0.0781	0.1808	0.784		
X_2X_4	0.087	0.9702	1	1	0.087	0.9702	2.37	6.87	0.1461	0.0201		*
X_3X_4	0.2704	2.66	1	1	0.2704	2.66	7.36	18.82	0.0168	0.0007	*	**
X_1	8.35	19.7	1	1	8.35	19.7	227.34	139.57	< 0.0001	< 0.0001	**	**
X_2	6.58	6.09	1	1	6.58	6.09	179.13	43.15	< 0.0001	< 0.0001	**	**
X_3	10.32	27.73	1	1	10.32	27.73	280.74	196.48	< 0.0001	< 0.0001	**	**
X_4	13.29	31.01	1	1	13.29	31.01	361.52	219.7	< 0.0001	< 0.0001	**	**
Residual	0.5145	1.98	14	14	0.0367	0.1411						
Lack of Fit	0.325	1.58	10	10	0.0325	0.1581	0.6859	1.6	0.7143	0.3448		
Pure Error	0.1895	0.3953	4	4	0.0474	0.0988						
Cor Total	33.9	106.54	28	28								

Note: ** indicates extremely significant difference (P < 0.01); * indicates significant difference (P < 0.05).

As shown in Table 3, the model F-value for dye-uptake and dye penetration rate was 64.90 and 52.92, respectively, and p-value < 0.0001 for both responses. These values indicate that the models were extremely significant and the quadratic polynomial regression models of dye-uptake (Y_1) and dye penetration rate (Y_2) proposed as in Eqs. (8) and (9) for the responses were valid for Ayous wood dye.

$$Y_1 = 14.18 - 0.04X_1 + 0.51X_2 + 0.06X_3 + 0.59X_4 + 0.26X_1X_2 - 0.29X_1X_3 - 0.10X_1X_4 + 0.14X_2X_3 - 0.15X_2X_4 - 0.26X_3X_4 - 1.13X_1^2 - 1.01X_2^2 - 1.26X_3^2 - 1.43X_4^2 \quad (8)$$

$$Y_2 = 22.11 + 1.10X_1 - 0.11X_2 - 0.12X_3 + 1.40X_4 + 0.27X_1X_2 - 0.31X_1X_3 - 1.04X_1X_4 - 0.05X_2X_3 - 0.49X_2X_4 + 0.82X_3X_4 - 1.74X_1^2 - 0.97X_2^2 - 2.07X_3^2 - 2.19X_4^2 \quad (9)$$

As can be seen from the p-value, X_2, X_4, X_1X_3, X_1^2, X_2^2, X_3^2 and X_4^2 had extremely significant effects on dye-uptake, X_1, X_4, X_1X_4, X_3X_4, X_1^2, X_2^2, X_3^2, X_4^2 had extremely significant influence on dye penetration rate, respectively. X_1X_2, X_3X_4 had significant influence on dye-uptake and X_2X_4 had significant influence on dye penetration rate, respectively. X_3, X_2X_3 had insignificant influence on dye-uptake and dye penetration rate. According to the results of variance analysis, it was concluded that the order of influence of each factor on dye-uptake within the scope of this experiment was as follows: accelerant mass fraction, dye concentration, dyeing time and temperature, while the order of influence of each factor on dye penetration rate was as follows:

accelerant mass fraction, temperature, dye concentration and dyeing time. From the Table 3, it can be seen that X_1X_3 was the interactive item that had a significant impact on dye-uptake, X_1X_4 and X_3X_4 were the interactive items that had a significant impact on dye penetration rate.

Effect of temperature and dyeing time

The effect of different levels of temperature and dyeing time on the dye-uptake can be evaluated from the response surface plot as shown in Fig. 7. The temperature was raised from 75 to 95 ^{o}C, and the dyeing time was raised from 6 to 10 h, the dye concentration remained constant at 0.3% and accelerant mass fraction was 2%. As the temperature increased to nearly 86.24 ^{o}C or the dyeing time increased to nearly 7.98 h, the dye-uptake was found to increase. After that, continued increase in temperature and dyeing time would result in a decrease in dye-uptake. The elliptical curve for contour at the bottom surface of the plot signifies that the interaction between the variables had a strong influence on the response factors (Anupam et al., 2011). The contour lines showed more concentric ellipses close to dyeing time, from which it can be inferred that the dyeing time has more influence on the dye-uptake.

Effect of temperature and accelerant mass fraction

According to Table 3, X_1X_4 and X_3X_4 have significant influence on dye penetration rate. The effect of the temperature and accelerant mass fraction on the dye penetration rate was evaluated at dye concentration of 0.3% and dyeing time of 8 h. Figure 8 shows the combined effect of temperature and accelerant mass fraction on the dye penetration rate. The dye penetration rate plot showed the peak in the center of the three-dimensional network. This illustrated that at low temperature and accelerant mass fraction, the dye penetration rate was less; as the temperature and accelerant were increased, the dye penetration showed an increasing trend. At a temperature of 85.85 ^{o}C and accelerant mass fraction of 2.24%, the dye penetration rate reached a maximum value of 22.38%. The contour lines showed more concentric ellipses close to accelerant mass fraction, from which it can be inferred that the accelerant mass fraction has more influence on the dye penetration rate.

Effect of dyeing time and accelerant mass fraction

The influence of dyeing time and accelerant mass fraction, in the range of 6–10 h and 1% – 3%, respectively, on the dye penetration rate at fixed temperature of 85 ^{o}C and dye concentration of 0.3% were observed. Figure 9 shows the combined effect of dyeing time and accelerant mass fraction on dye penetration rate. The dye penetration rate plot showed the peak in the center of the three-dimensional network. The maximum dye penetration rate was observed to be 22.33% for a dyeing time of 8.01 h and an accelerant mass fraction of 2.25%.

Optimization and validation

A multiple response approach was applied for optimization of any combination of the six goals viz. temperature, dye concentration, dyeing time, accelerant mass fraction, dye-uptake and dye penetration rate. Finally, a set of conclusions was drawn from the optimization results as shown in Table 4. The goal was set for maximum dye-uptake and dye penetration rate, keeping the temperature in range, dye concentration in range, dyeing time in range, and accelerant mass fraction in range, the desirability function obtained was 0.970. The outcome of the model gives a set of factors as shown in Table 4.

The optimum dyeing conditions were temperature of 86.03 ^{o}C, dye concentration of 0.31%, dyeing time of 8 h and accelerant mass fraction of 2.23%. The dye-uptake and dye penetration rate predicted by the model were 14.28% and 22.34%, respectively. Three experiments were carried out under the optimum conditions. The actual dye-uptake was 14.50% and the actual dye penetration rate was 22.59%. The relative errors with the theoretical values were 1.57% and 1.12%, respectively, which shows that the model was reasonable and effective.

Table 4
Optimization results for dye-uptake and dye penetration rate

Factors				Response					
X_1	X_2	X_3	X_4	Y_1			Y_2		
				Predicted	Actual	Error	Predicted	Actual	Error
86.03	0.31	8.00	2.23	14.28	14.50	1.57	22.34	22.59	1.12

Conclusion

In present work, the effect of temperature, dye concentration, dyeing time and accelerant mass fraction on the dye-uptake and dye penetration rate of Ayous wood in the dyeing process with acid dye was studied. The following outcomes of the experiment were noticed:

(1) With the increase of temperature, dye concentration, dyeing time and accelerant mass fraction, the dye-uptake and dye penetration rate of Ayous wood rose first and then fell. Appropriate conditions were beneficial to dye uptake and penetration. Excessive dye and accelerant concentration would cause dye aggregation, which is not conducive to dye diffusion and penetration.

(2) The response surface methodology was extended to study the optimization of dyeing process. The results of ANOVA showed that the value of R^2, adj. R^2, Pred. R^2 were all close to the ideal, Adeq. precision of models were greater than 4.0, and p-value of models were less than 0.01, so the quadratic models were significant.

(3) The optimum dye-uptake and dye penetration rate were found to be 14.28% and 22.34%, respectively, at temperature of 86.03 ^oC, dye concentration of 0.31%, dyeing time of 8 h and accelerant mass fraction of 2.23%.

Declarations

Acknowledgements: The authors are grateful to Prof. Jinlin Wang who helped to establish the experimental protocol.

References

1. Ahmad, A. A.,Hameed, B. H. (2010). Effect of preparation conditions of activated carbon from bamboo waste for real textile wastewater. *Journal of Hazardous Materials*, 173(1), 487-493. doi:10.1016/j.jhazmat.2009.08.111.
2. Amini, M.,Younesi, H. (2009). Biosorption of Cd(II), Ni(II) and Pb(II) from Aqueous Solution by Dried Biomass of Aspergillus niger: Application of Response Surface Methodology to the Optimization of Process Parameters (10.1002/clen.200900090). *CLEAN – Soil, Air, Water*, 37(10), 776-786. doi:https://doi.org/10.1002/clen.200900090.
3. Antony, J. (2014). Design of experiments for engineers and scientists. London: Elsevier.
4. Anupam, K., Dutta, S., Bhattacharjee, C.,Datta, S. (2011). Adsorptive removal of chromium (VI) from aqueous solution over powdered activated carbon: Optimisation through response surface methodology. *Chemical Engineering Journal*, 173(1), 135-143. doi:https://doi.org/10.1016/j.cej.2011.07.049.
5. Azargohar, R.,Dalai, A. K. (2005). Production of activated carbon from Luscar char: Experimental and modeling studies. *Microporous and Mesoporous Materials*, 85(3), 219-225. doi:https://doi.org/10.1016/j.micromeso.2005.06.018.
6. Bao, M., Huang, X., Zhang, Y., Yu, W.,Yu, Y. (2016). Effect of density on the hygroscopicity and surface characteristics of hybrid poplar compreg. *Journal of Wood Science*, 62(5), 441-451. doi:10.1007/s10086-016-1573-4.
7. Borrega, M., Ahvenainen, P., Serimaa, R.,Gibson, L. (2015). Composition and structure of balsa (Ochroma pyramidale) wood. *Wood Science and Technology*, 49(2), 403-420. doi:10.1007/s00226-015-0700-5.

8. Box, G. E. P.,Wilson, K. B. (1951). On the Experimental Attainment of Optimum Conditions. *Journal of the Royal Statistical Society. Series B (Methodological)*, 13(1), 1-45. http://www.jstor.org/stable/2983966.
9. Chen, Y., Lu, R.,Zheng, R. (2000). Effects of *Paulownia* Veneer Dyeing Factors to the Chromatism. *China Wood Industry*, 14(4), 10-12.
10. Comstock, G. L. (2007). Directional Permeability Of Softwoods. *Wood and fiber science*, 1, 283-289.
11. Convert, R., Schacher, L.,Viallier, P. (2000). An expert system for the dyeing recipes determination. *Journal of Intelligent Manufacturing*, 11(2), 145-155. doi:10.1023/A:1008986732187.
12. Danish, M., Hashim, R., Ibrahim, M. N. M.,Sulaiman, O. (2014a). Optimized preparation for large surface area activated carbon from date (Phoenix dactylifera L.) stone biomass. *Biomass and Bioenergy*, 61, 167-178. doi:10.1016/j.biombioe.2013.12.008.
13. Danish, M., Hashim, R., Mohamad Ibrahim, M. N.,Sulaiman, O. (2014b). Response surface methodology approach for methyl orange dye removal using optimized Acacia mangium wood activated carbon. *Wood Science and Technology*, 48(5), 1085-1105. doi:10.1007/s00226-014-0659-7.
14. Das, A.,Mishra, S. (2017). Removal of textile dye reactive green-19 using bacterial consortium: Process optimization using response surface methodology and kinetics study. *Journal of Environmental Chemical Engineering*, 5(1), 612-627. doi:10.1016/j.jece.2016.10.005.
15. Deng, H.,Liu, Y. (2010) 'Study on Environmental-Friendly Dyeing Processes of Fast-Growing Plantation Veneers' *2010 4th International Conference on Bioinformatics and Biomedical Engineering*. 18-20 June 2010. pp. 1-4.
16. Deng, S., Wang, C., Lin, J.,Chen, X. (2019). Optimization of the freeze-thaw cycle pretreatment process of Chinese fir wood using the response surface method. *Journal of Forest and Environment*, 39(06), 647-653. doi:10.13324/j.cnki.jfcf.2019.06.013.
17. Duan, X. (2002). Wood Color Control Technology. Beijing: China Building Materials Press.
18. Ghaedi, M., Khafri, H. Z., Asfaram, A.,Goudarzi, A. (2016). Response surface methodology approach for optimization of adsorption of Janus Green B from aqueous solution onto ZnO/Zn(OH)2-NP-AC: Kinetic and isotherm study. *Spectrochimica Acta Part A: Molecular and Biomolecular Spectroscopy*, 152, 233-240. doi:10.1016/j.saa.2015.06.128.
19. Hazir, E.,Ozcan, T. (2019). Response Surface Methodology Integrated with Desirability Function and Genetic Algorithm Approach for the Optimization of CNC Machining Parameters. *Arabian Journal for Science and Engineering*, 44(3), 2795-2809. doi:10.1007/s13369-018-3559-6.
20. Hu, J., Fan, W., Li, L.,Guo, H. (2016). Optimal Dyeing Process for Maple Veneer. *Journal of Northeast Forestry University*, 44(08), 68-72.
21. Hu, J., Liu, Y.,Wu, Z. (2020). Structural Color for Wood Coloring: A Review. *Bioresources*, 15(4), 9917-9934.
22. Jardine, D. I., Blanc-Jolivet, C., Dixon, R. R. M., Dormontt, E. E., Dunker, B., Gerlach, J., et al. (2016). Development of SNP markers for Ayous (Triplochiton scleroxylon K. Schum) an economically important tree species from tropical West and Central Africa. *Conservation Genetics Resources*, 8(2), 129-139. doi:10.1007/s12686-016-0529-8.
23. Jaxel, J., Amer, H., Bacher, M., Roller, A., Guggenberger, M., Zwirchmayr, N. S., et al. (2020). Facile synthesis of 1-butylamino- and 1,4-bis(butylamino)-2-alkyl-9,10-anthraquinone dyes for improved supercritical carbon dioxide dyeing. *Dyes and Pigments*, 173, 107991. doi:10.1016/j.dyepig.2019.107991.
24. Khataee, A. R., Kasiri, M. B.,Alidokht, L. (2011). Application of response surface methodology in the optimization of photocatalytic removal of environmental pollutants using nanocatalysts. *Environmental Technology*, 32(15), 1669-1684. doi:10.1080/09593330.2011.597432.
25. Knudson, R.,Brunette, G. (2015). Evaluation of Canadian Prairie-Grown Hybrid Poplar for High Value Solid Wood Products. *The Forestry Chronicle*, 91(02), 141-149. doi:10.5558/tfc2015-025.
26. Li, Y., Liu, Y., Wang, F.,Gang, G. (2011). Controlling Factors of Wood Permeability and Its Improving Measures. *Scientia Silvae Sinicae*, 47(5), 131-139.

27. Liu, M., Lyu, S., Peng, L., Cai, L., Huang, Z.,Lyu, J. (2021a). Improvement of Toughness and Mechanical Properties of Furfurylated Wood by Biosourced Epoxidized Soybean Oil. *ACS Sustainable Chemistry & Engineering*, 9(24), 8142-8155. doi:10.1021/acssuschemeng.1c01358.
28. Liu, M., Lyu, S., Peng, L., Lyu, J.,Huang, Z. (2021b). Radiata pine fretboard material of string instruments treated with furfuryl alcohol followed by tung oil. *Holzforschung*, 75(5), 480-493. doi:10.1515/hf-2020-0048.
29. Liu, Y., Hu, J., Gao, J., Guo, H., Chen, Y., Cheng, Q., et al. (2015). Wood Veneer Dyeing Enhancement by Ultrasonic-assisted Treatment (Review). *Bioresources*, 10(1), 1198-1212. <Go to ISI>://WOS:000351941000097.
30. Liu, Y., Yu, Z., Zhang, Y., Qi, C., Tang, R., Zhao, B., et al. (2020). Microbial dyeing-infection behavior and influence of *Lasiodiplodia theobromae* in poplar veneer. *Dyes and Pigments*, 173, 107988. doi:10.1016/j.dyepig.2019.107988.
31. López, G., Basterra, L.-A.,Acuña, L. (2018). Infrared thermography for wood density estimation. *Infrared Physics & Technology*, 89, 242-246. doi:https://doi.org/10.1016/j.infrared.2018.01.015.
32. Lv, J., Bao, F., Jiang, X.,Zhao, M. (1994). Effect of Steaming on The Permeability of Wood. *Scientia Silvae Sinicae*, 30(4), 352-357+386-388.
33. Machová, D., Baar, J., Paschová, Z., Pařil, P., Křenková, J.,Kúdela, J. (2019). Color changes and accelerated ageing in oak wood treated with ammonia gas and iron nanoparticles. *European Journal of Wood and Wood Products*, 77(4), 705-716. doi:10.1007/s00107-019-01406-x.
34. Meng, F., Wu, B., Yu, Y.,Yu, W. (2016a). Effect of Thicker Veneers on Properties of Laminated Veneer Lumber. *China Wood Industry*, 30(03), 5-8.
35. Meng, F., Wu, B., Yu, Y.,Yu, W. (2016b). Manufacturing Technology and Application of Laminated Veneer Lumber Made with Thicker Veneers. *China Wood Industry*, 30(04), 13-16.
36. Mikhailovskaya, A. P., Dashchenko, N. V., Dyankova, T. Y.,Dmitrieva, I. B. (2001). Enhancing the Effect of Surfactants in Dyeing of Aramid Fibres. *Fibre Chemistry*, 33(4), 271-274.
37. Ndukwu, M. C., Bennamoun, L., Simo-Tagne, M., Ibeh, M. I., Abada, U. C.,Ekop, I. E. (2021). Influence of drying applications on wood, brick and concrete used as building materials: a review. *Journal of Building Pathology and Rehabilitation*, 6(1), 24. doi:10.1007/s41024-021-00119-0.
38. Nguyen, N., Ozarska, B., Fergusson, M.,Vinden, P. (2018a). Comparison of two dye uptake measurement methods for dyed wood veneer assessment. *European Journal of Wood and Wood Products*, 76(6), 1757-1759. doi:10.1007/s00107-018-1344-6.
39. Nguyen, N. B., Ozarska, B., Fergusson, M.,Vinden, P. (2018b). Investigation into the Optimal Dyeing Method for Bluegum (*Eucalyptus globulus*) Veneer. *BioResources*, 13(3), 6444-6464. https://ojs.cnr.ncsu.edu/index.php/BioRes/article/view/BioRes_13_3_6444_Nguyen_Investigation_Optimal_Dyeing_Method.
40. Nouemsi Soubgui, E., Tene Fongang, R. T., Kamseu, E., Oum Lissouck, R., Andreola, F., Boubakar, L., et al. (2021). Microstructure and physico-chemical transformation of some common woods from Cameroon during drying. *Journal of Thermal Analysis and Calorimetry*, 145(6), 3003-3018. doi:10.1007/s10973-020-09890-7.
41. Rowell, R. M. (2012). Handbook of Wood Chemistry and Wood Composites. Boca Raton: CRC Press.
42. Ryan, T. P. (2007). Modern Experimental Design. John Wiley & Sons.
43. Singh, V., Soni, A.,Singh, R. (2016). Process Optimization Studies of Malachite Green dye Adsorption onto Eucalyptus (Eucalyptus globulus) Wood Biochar using Response Surface Methodology. *Oriental Journal of Chemistry*, 32(5), 2621-2631. doi:10.13005/ojc/320534.
44. Song, X.,Shen, Y. (2009). Dyeing with the reactive dyes. Beijing: China Textile Press.
45. Togue Kamga, F. (2018). Modeling adsorption mechanism of paraquat onto Ayous (Triplochiton scleroxylon) wood sawdust. *Applied Water Science*, 9(1), 1. doi:10.1007/s13201-018-0879-3.
46. Vakhitova, N. A.,Safonov, V. V. (2003). Effect of Chitosan on the Efficiency of Dyeing Textiles with Active Dyes. *Fibre Chemistry*, 35(1), 27-28. doi:10.1023/A:1023819521538.

47. Wang, C., Deng, S.,Lin, J. (2018a). Dyeing properties of *Cunninghamia lanceolata* wood with acid dye. *Journal of Forest and Environment*, 38(1), 111-117. doi:10.13324/j.cnki.jfcf.2018.01.018.
48. Wang, X., Yu, Z., Zhang, Y., Qi, C.,Chang, W.-l. (2018b). Evaluation of ultrasonic-assisted dyeing properties of fast-growing poplar wood treated by reactive dye based on grey system theory analysis. *Journal of Wood Science*, 64(6), 861-871. doi:10.1007/s10086-018-1768-y.
49. Wang, X., Zhang, Y., Yu, Z.,Qi, C. (2017). Properties of fast-growing poplar wood simultaneously treated with dye and flame retardant. *European Journal of Wood and Wood Products*, 75(3), 325-333. doi:10.1007/s00107-016-1142-y.
50. Witek-Krowiak, A., Chojnacka, K., Podstawczyk, D., Dawiec, A.,Pokomeda, K. (2014). Application of response surface methodology and artificial neural network methods in modelling and optimization of biosorption process. *Bioresource Technology*, 160, 150-160. doi:10.1016/j.biortech.2014.01.021.
51. Yang, L., Liu, H., Cai, Y.,Wu, Z. (2019). A novel method of studying the collapsed cell of eucalyptus wood using X-ray CT scanning. *Drying Technology*, 37(12), 1597-1604. doi:10.1080/07373937.2018.1519572.
52. Yusop, M. F. M., Ahmad, M. A., Rosli, N. A.,Manaf, M. E. A. (2021). Adsorption of cationic methylene blue dye using microwave-assisted activated carbon derived from acacia wood: Optimization and batch studies. *Arabian Journal of Chemistry*, 14(6), 103122. doi:https://doi.org/10.1016/j.arabjc.2021.103122.
53. Zhang, Y., Yu, Z.,Wu, X. (2015). Comparison among Parameters Affecting Vertical Vacuum Dyeing of Populus cathayana Rehd. *Forest Products Journal*, 65(3-4), 123-128. doi:10.13073/FPJ-D-14-00064.
54. Zhao, G., Wang, D., Li, X., He, L., Shi, W., Zhao, G., et al. (1993). The permeation process of dye liquor in wood. *Journal of Northeast Forestry University*, 21(5), 54-59.
55. Zhu, T., Sheng, J., Chen, J., Ren, K., Wu, Z., Wu, H., et al. (2021). Staining of wood veneers with anti-UV property using the natural dye extracted from Dalbergia cohinchinensis. *Journal of Cleaner Production*, 284, 124770. doi:10.1016/j.jclepro.2020.124770.

Figures

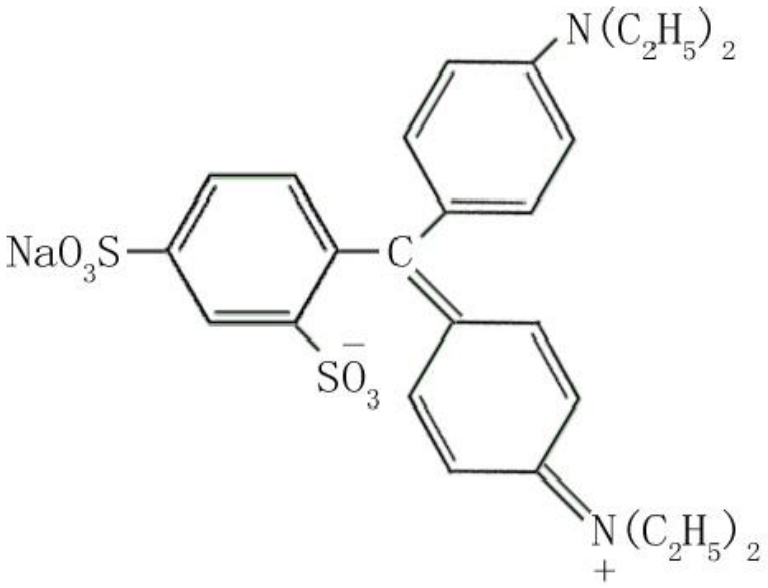


Figure 1

Molecular structural formula of acid blue V

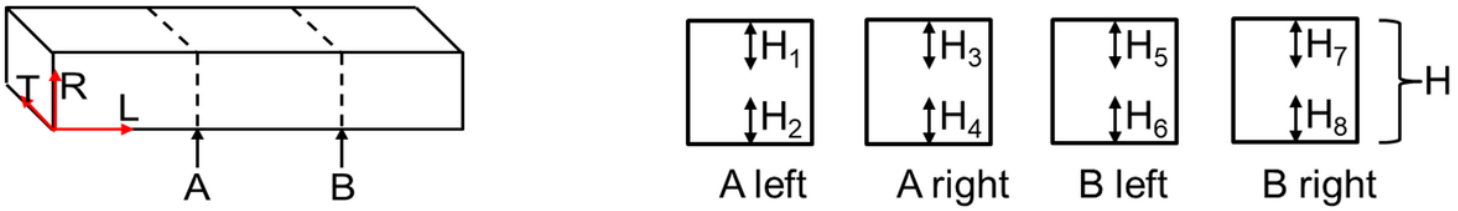


Figure 2

The measurement of radial dye penetration of samples

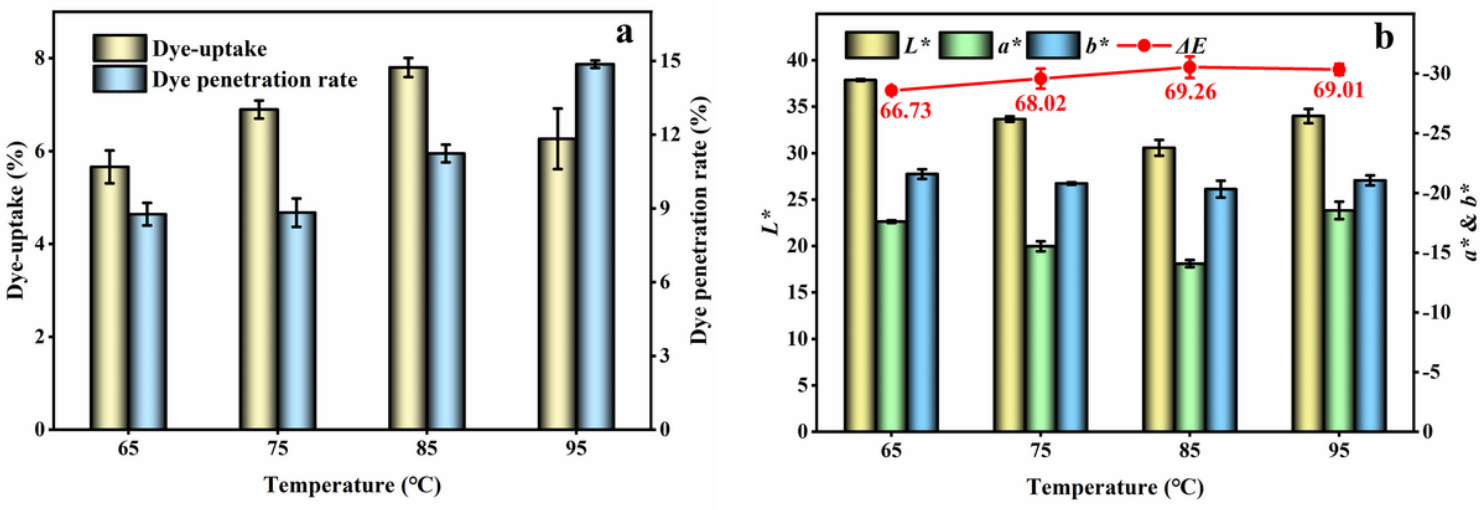


Figure 3

Effect of temperature on the dyeing properties of Ayous wood (a) Dye-uptake and radial dye penetration rate; (b) Wood surface color parameters

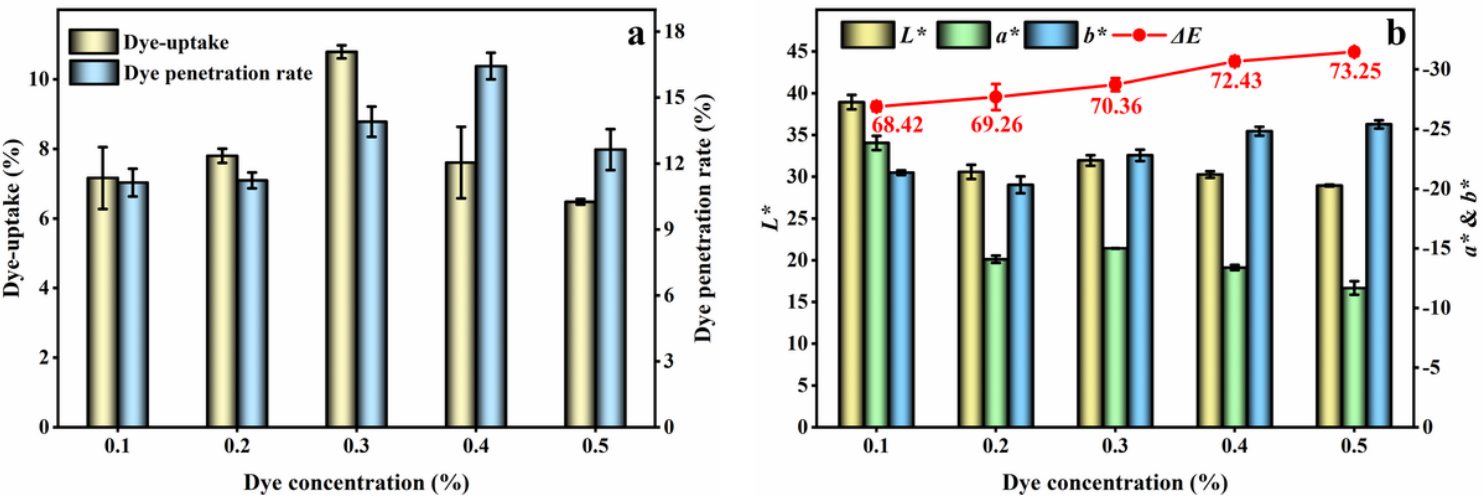


Figure 4

Effect of dye concentration on the dyeing properties of Ayous wood (a) Dye-uptake and radial dye penetration rate; (b) Wood surface color parameters

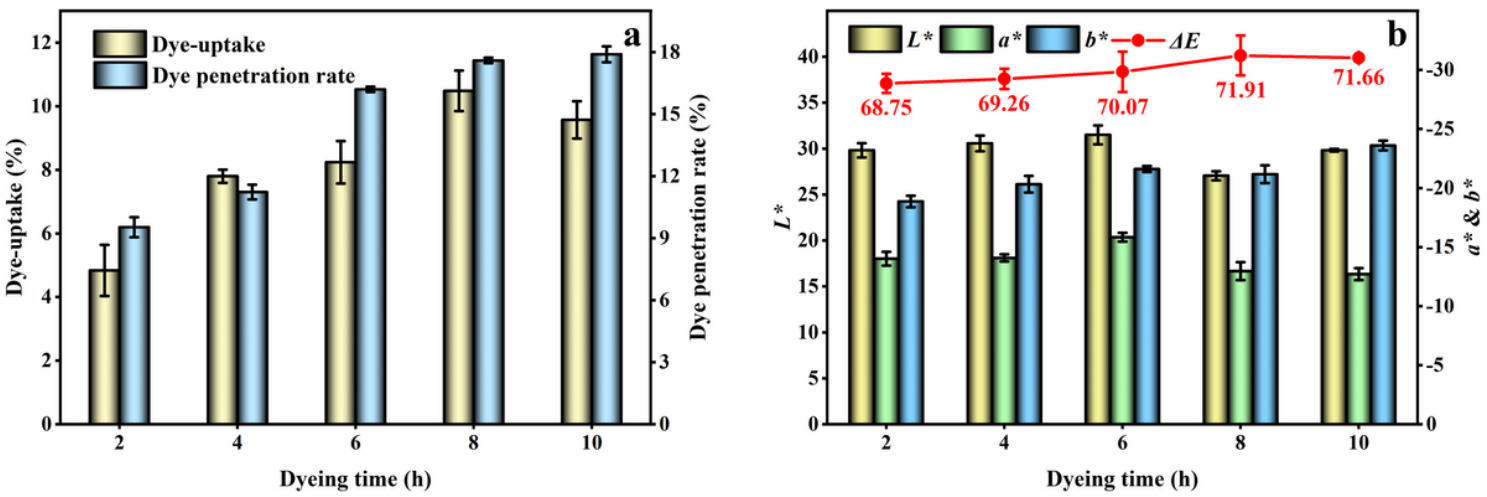


Figure 5

Effect of dyeing time on the dyeing properties of Ayous wood (a) Dye-uptake and radial dye penetration rate; (b) Wood surface color parameters

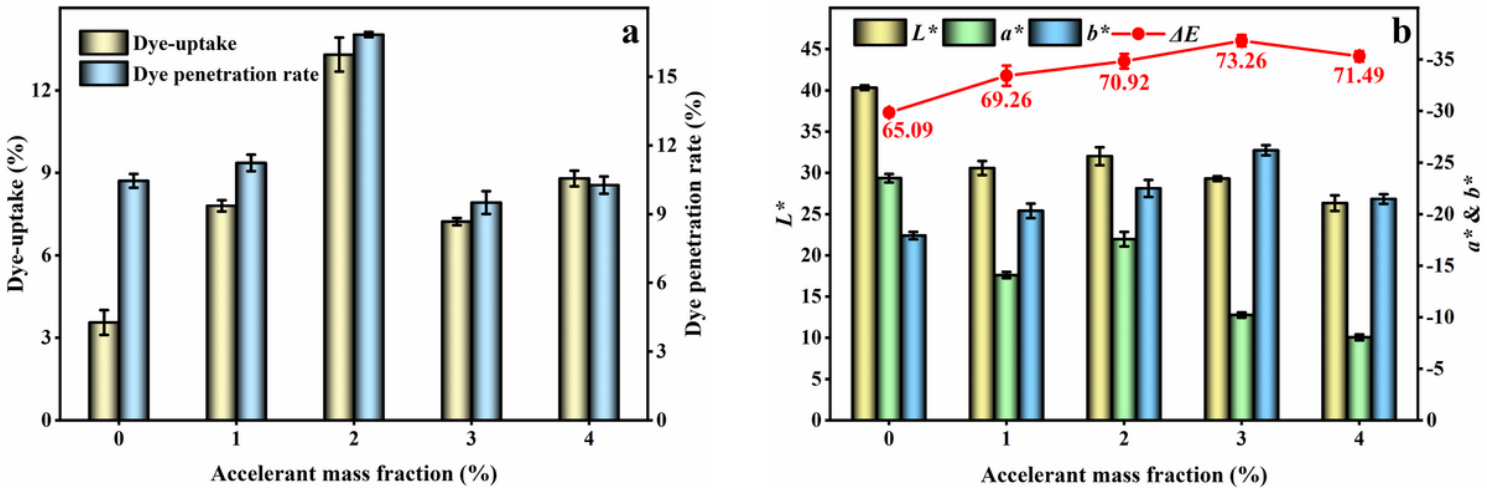


Figure 6

Effect of accelerant mass fraction on the dyeing properties of Ayous wood (a) Dye-uptake and radial dye penetration rate; (b) Wood surface color parameters

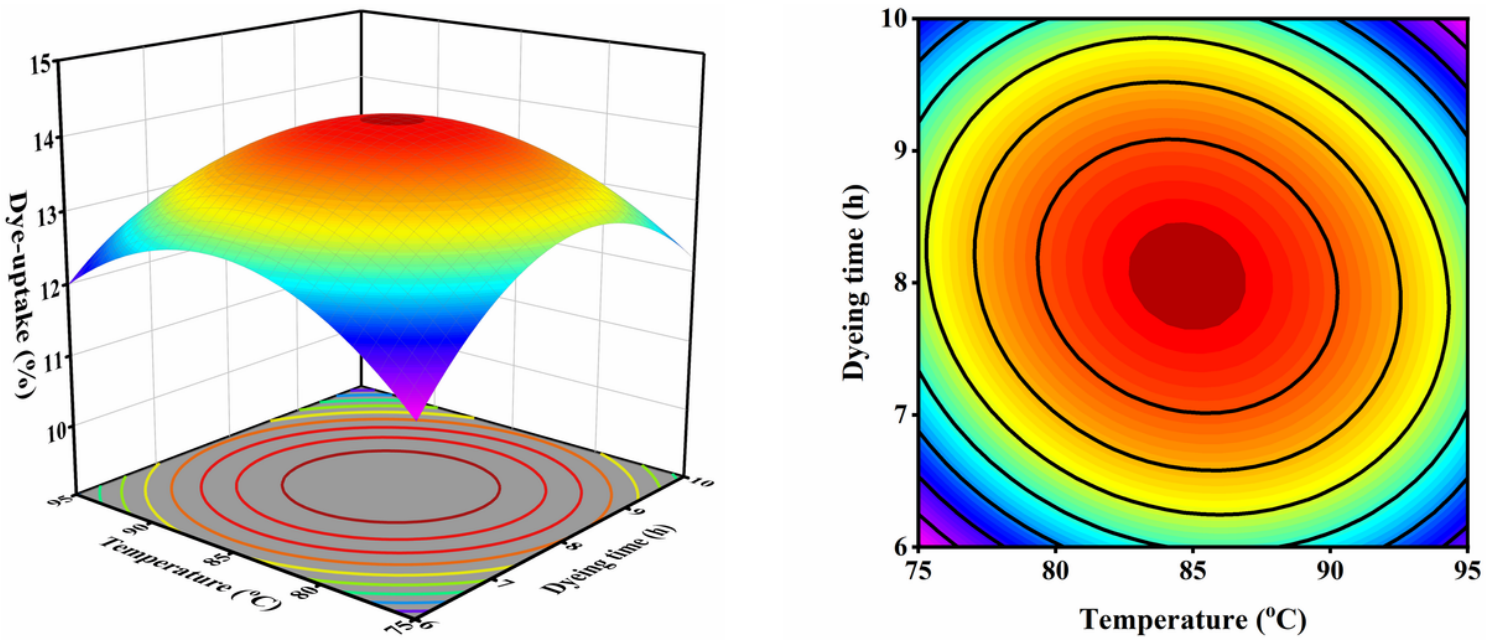


Figure 7

Interaction effects of temperature and dyeing time on the dye-uptake

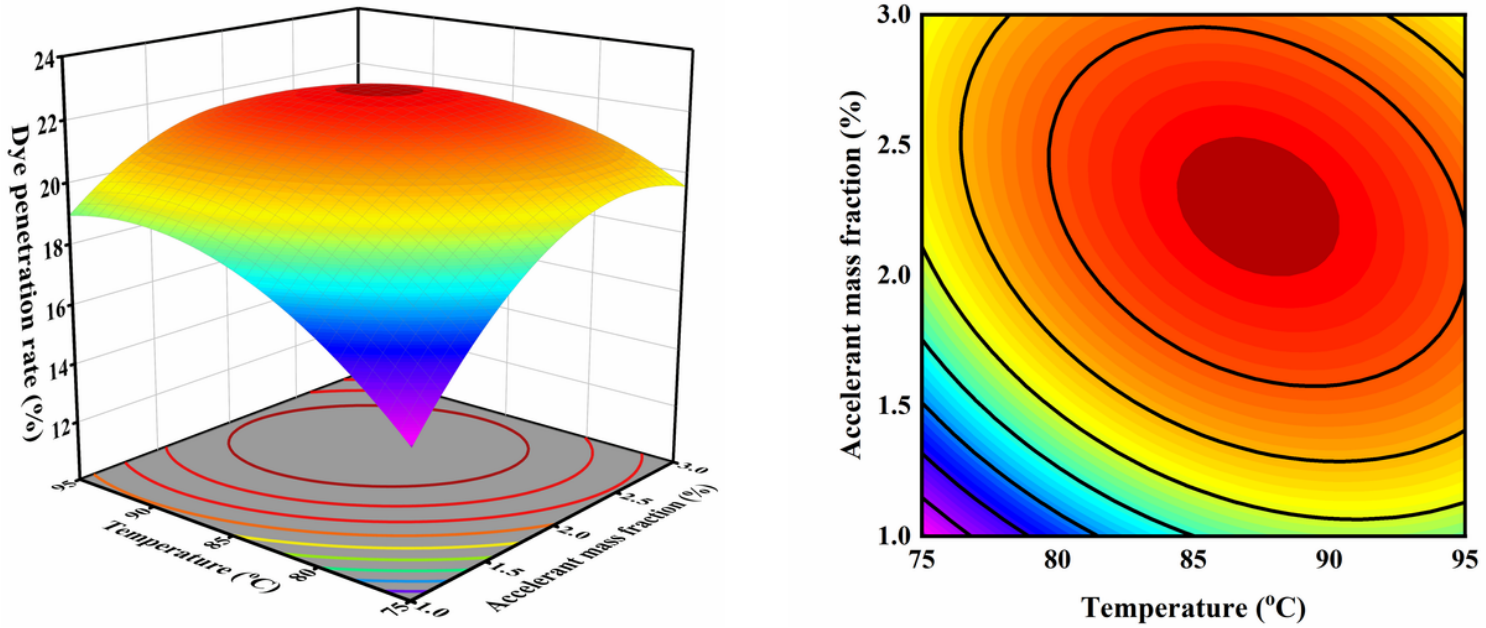


Figure 8

Interaction effects of temperature and accelerant mass fraction on the dye penetration rate

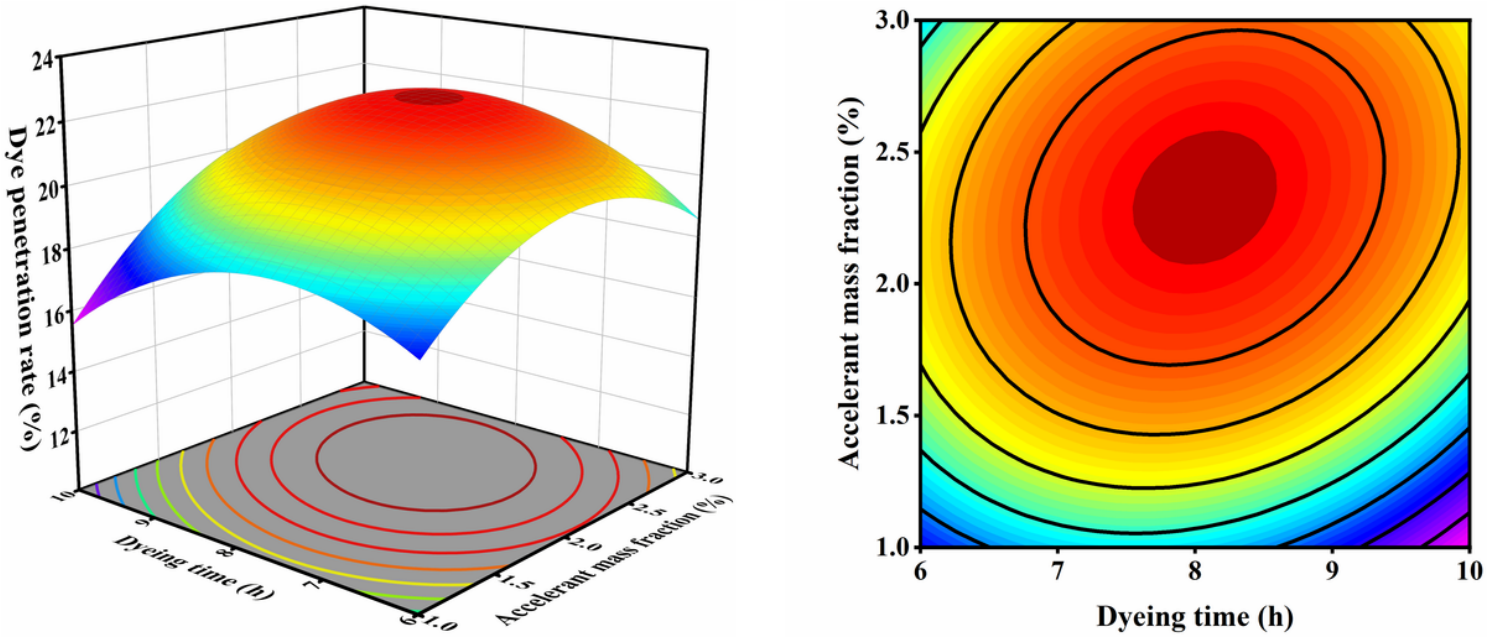


Figure 9

Interaction effects of dyeing time and accelerant mass fraction on the dye penetration rate